International Communications in Heat and Mass Transfer 74 (2016) 82–90

Contents lists available at ScienceDirect

International Communications in Heat and Mass Transfer

journal homepage: www.elsevier.com/locate/ichmt

A reliable model to predict thermal conductivity of unsaturated weathered granite soils☆

Gyu-Hyun Go [a], Seung-Rae Lee [b,*], Young-Sang Kim [c]

[a] Convergence Research Planning Division, KICT, Goyang 411-712, Republic of Korea
[b] Department of Civil and Environmental Engineering, KAIST, Daejeon 34141, Republic of Korea
[c] Department of Marine and Civil Engineering, Chonnam National University, Yeosu 59626, Republic of Korea

ARTICLE INFO

Available online 1 February 2016

Keywords:
Weathered granite soil
Effective thermal conductivity
Unsaturated condition
Statistical–physical model
Artificial neural network

ABSTRACT

The aim of this study is to present a new empirical model to predict thermal conductivity, based on experimental databases that might be particularly applicable to unsaturated weathered granite soils. To establish the experimental databases, a number of thermal conductivity tests were conducted using a new probe system combined with a volumetric pressure extractor. Thereby, 162 data were collected and applied to the prediction model. The prediction model has two empirical coefficients that determine the shape of a graph, and it is not easy to determine these coefficients unless experiments are conducted. Thus, in this paper, we propose using an artificial neural network model to obtain these empirical coefficients without experiments, given only information on the soil properties. Moreover, to evaluate the applicability of the trained network model, it was tested for data sets that had not been introduced during the training stage. According to the verification results, the trained network model presents reasonable prediction results ($R^2 = 0.9046$), even for the new testing data. In addition, the model traces the measured data curve with fairly good agreement, depending on a sample's porosity, regional characteristics, and degree of saturation.

1. Introduction

Recently, the depletion of fossil fuel sources and rising energy consumption, have emerged as serious problems for global society. To achieve energy savings and reduce greenhouse gases, the use of renewable energy sources is becoming inevitable all over the world. In particular, Ground Source Heat Pump (GSHP) systems making use of renewable energy stored in the ground have been recognized as a clean, efficient way to enhance space heating and cooling of buildings. They use relatively constant ground temperatures as a heat reservoir: a heat source in winter and a heat sink in summer. Though a vertical loop [1] has often been the choice for GSHP systems, this approach is facing a major obstacle due to its high initial construction cost, which comes from the required drilling operation [2–4]. For this reason, attention is shifting to GSHP systems using shallow grounds. A typical example of a shallow GSHP system is an energy pile and horizontal loop system. The energy pile has been used as part of the ground heat exchangers to overcome the initial cost of conventional vertical loop systems [5–8]. This innovative idea has led to notable progress in the field of GSHP systems and has become particularly attractive to developers in urban areas. This is because it offers the lowest total cost while offering the highest renewable contribution, and the lowest spatial requirements [9]. In addition, horizontal loop systems are often preferred over vertical loop if the site has adequate space. Owing to the lower initial installation costs, the use of horizontal loops can provide a viable alternative solution that reaches a good compromise between efficiency and cost [10–12].

In most cases, all or some parts of the ground heat exchanger in shallow GSHP systems are located above the ground water table (GWT). This means that the shallow ground above the GWT consists of three-phase soils: solid mineral components, water, and air. Because three-phase soils are unsaturated (with water), the thermal properties of the ground relatively near the surface can be affected by unsaturated soil behaviors. Hence, the performance of GSHPs can also be influenced by complex soil behavior at shallow depths [13–14]. Thus, there have been extensive studies on the prediction of thermal conductivity of unsaturated soils, based on empirical or theoretical approaches. For example, Kersten [15] proposed an empirical model in 1949, and it is considered one of the first approaches to predict the thermal conductivity of frozen soils. After that, Johansen [16] suggested another empirical model having a logarithmic form, obtained by regression analysis. Donazzi et al. [17] investigated the thermal and hydrological characteristics of the soil surrounding buried cables and proposed an empirically derived model. Farouki [18] reviewed several methods for prediction of the effective thermal conductivity of frozen soils, and provided an extensive collection of experimental data for unfrozen and frozen soils. Cote and Konrad [19] modified Johansen's model to eliminate the

☆ Communicated by W.J. Minkowycz.
* Corresponding author.

http://dx.doi.org/10.1016/j.icheatmasstransfer.2016.01.009
0735-1933/

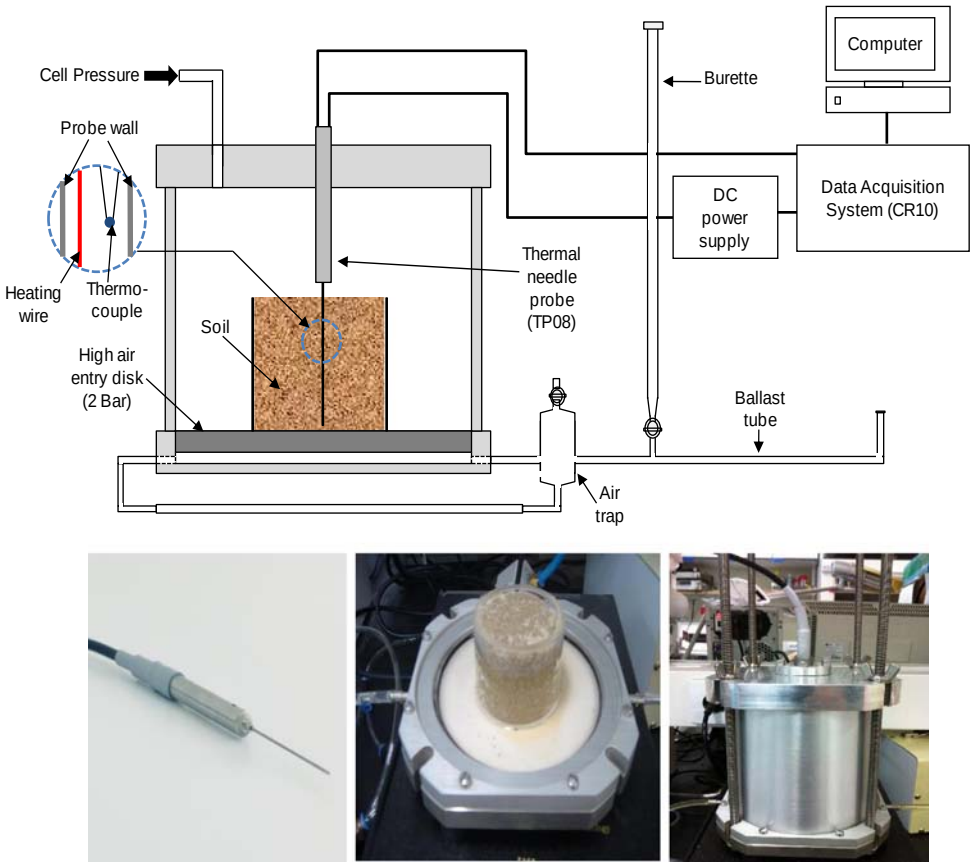

Fig. 1. Schematic diagram of thermal conductivity test for unsaturated soils [36].

logarithmic dependence on the saturation ratio, which distorted predictions at low degrees of saturation. They suggested three empirical parameters that could consider the effect of particle shape and soil texture. Lu et al. [20] also modified Johansen's model and suggested several empirical parameters for sandy soils. Chen [21] proposed an empirical equation, based on 80 needle-probe tests on sands with a wide range of particle sizes, saturation ratios, and void ratios. In addition to above models, there are simpler mixed models based upon such as arithmetic, harmonic, and geometric means. These are statistical models containing both fixed effects and random effects, and are known to be particularly useful in computation of multi-phase thermal conductivity.

An analytical solution was attempted by Germant [22]; he evaluated the thermal conductivity of an array of chipped spherical particles with circular areas of contact between them. After that, De Vries [23] suggested a soil thermal conductivity model based on Maxwell's equations for the electrical conductivity of uniform spheres dispersed within a continuous fluid. A previous model [23] was extended by Penner [24] to accommodate frozen soils after extensive experiments [25]. Gori

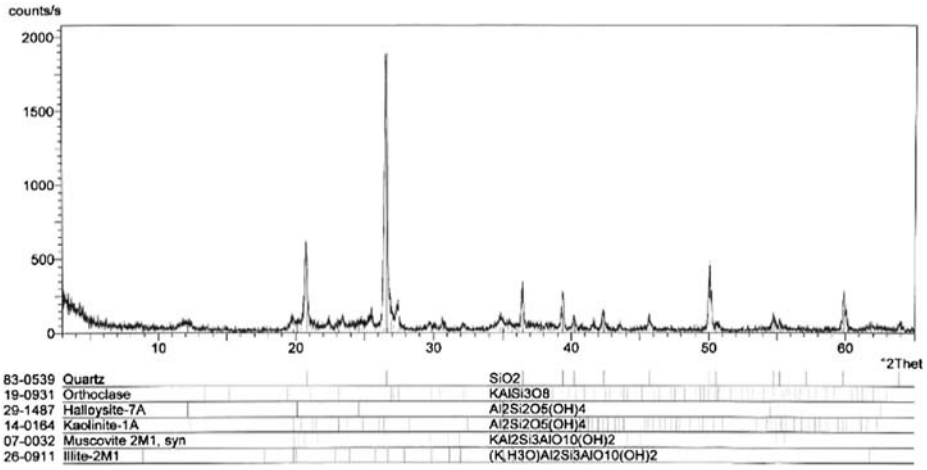

Fig. 2. Results of mineral quantitative analysis using X-ray diffusion (XRD) method.

Table 1
Results of mineral quantitative analysis and particle thermal conductivity.

Soil	Mineral portion (%)[a]								λ_p[b] (W/m K)
	Quartz (7.69)	Microcline (2.49)	Albeit (1.96)	Kaolin $(3.0)^+$	Orthoclase (2.32)	Muscovite (3.48)	Illite $(3.0)^+$	Chlorite (5.15)	
SJ	25.6	27.6	31.7	1.1	–	7.9	5.1	–	3.572
KP	28.6	19.0	28.5	9.0	–	6.8	–	1.1	3.491
KI	38.3	17.0	10.0	13.9	–	12.2	7.5	1.1	4.216
KT	32.9	19.3	5.0	26.2	–	4.9	5.5	3.0	4.036
BG	38.5	–	23.5	17.9	19.2	–	–	0.6	3.875
SY	28.2	21.8	24.6	13.8	–	5.9	4.2	0.8	3.504
CD	40.7	–	–	30.8	17.4		11.1		6.044
CY	43.9	–	13.8	25.5	16.8	–		–	4.750

Each mineral's thermal conductivity was obtained from the literature [38].
[a] Provided by KIGAM (Korea Institute of Geoscience and Mineral Resources).
[b] λ_p: Particle thermal conductivity.

[26] originally proposed a cubic-cell model for unsaturated frozen soils and it was tested with experimental data of two-phase media [27–28]. Since then, Tarnawski [29] proposed a modification that made the model valid for unfrozen soils. Gori and Corasaniti [30] considered the effect of increasing thermal conductivity of the gas phase (air) due to humidity in the model to improve its use at high temperature. Moreover, Haigh [31] developed an analytical solution based on unidirectional heat flow through a three-phase soil element, and it was validated against a database of test measurements. Recently, Gori and Corasaniti [32] presented a new theoretical model with quasi-spherical solid grain, extending the original proposal for two-phase media in [33] and presented in preliminary form in [34].

To summarize, many previous studies have dealt with evaluation of the thermal conductivity of unsaturated multi-phase soil. Even though there has been great progress by these many researchers, some challenges remain. Because most empirical models are applicable to certain types of soil (e.g., sandy or coarse materials), proof is needed to show that they are also applicable to other kinds of soil. Also, because theoretical models tend to be valid for a limited range of soil porosity (or degree of saturation), they encounter difficulties in practical use if the soil conditions exceed to their valid range.

In this paper, a new empirical model to predict thermal conductivity is presented, based on experimental databases that appear particularly applicable to modeling of unsaturated weathered granite soils. First, to establish the experimental databases, a number of thermal conductivity tests were conducted using a new probe system combined with a volumetric pressure extractor. Thereby, 162 data were collected and applied to the prediction model. The prediction model so developed has two empirical coefficients that determine the shape of graph. However, these coefficients are difficult to determine without conducting experiments. Accordingly, in this paper we propose the use of an artificial neural network model that can directly obtain the empirical coefficients, without experiments, given just the information on the soil properties. Then we evaluated the applicability of the model by testing with the data sets that had not been introduced during the training stage.

Table 2
Previous prediction models applied to thermal conductivity test analysis.

Model	Prediction formula	Remark
Kersten [15]	$\lambda = 0.1442(0.7\log w + 0.4)\cdot 10^{0.6243\rho_d}$	ρ_d in g/cm^3
Johansen [16]	$\lambda = (\lambda_{sat} - \lambda_{dry})\cdot(0.7\ ,\log S_r + 1.0)$, where $\lambda_{sat} = \lambda_p^{1-n}\lambda_w^n$, $\lambda_{dry} = (0.137\rho_d + 64.7)/(2700 - 0.947\rho_d) \pm 20\%$	ρ_d in kg/m^3
Côté and Konrad [19]	$\lambda = (\lambda_{sat} - \lambda_{dry})\cdot[kS_r/(1 + (k-1)S_r)] + \lambda_{dry}$, where k = empirical parameter, $\lambda_{dry} = \chi 10^{-\eta n}\chi = 0.75$ for soil, η = particle shape parameter, n = porosity	Coarse-fine grained soil
Lu et al. [20]	$\lambda = (\lambda_{sat} - \lambda_{dry})\cdot(\ ,\exp\{\alpha[1 - S_r^{\alpha-1.33}]\})$, where $\alpha = 0.96$ for coarse soil, $\lambda_{dry} = -0.56n + 0.51$, n = porosity	Coarse grained soil
Geometric mean model	$\lambda = \prod\lambda_{m_j}^{x_j}$, x = volume fraction, j = soil grain, pore water, and pore air	Theoretical model

w: moisture content, S_r: degree of saturation, λ_p: thermal conductivity of soil particle, λ_w: thermal conductivity of water (= 0.57 Wm^{-1} K^{-1}).

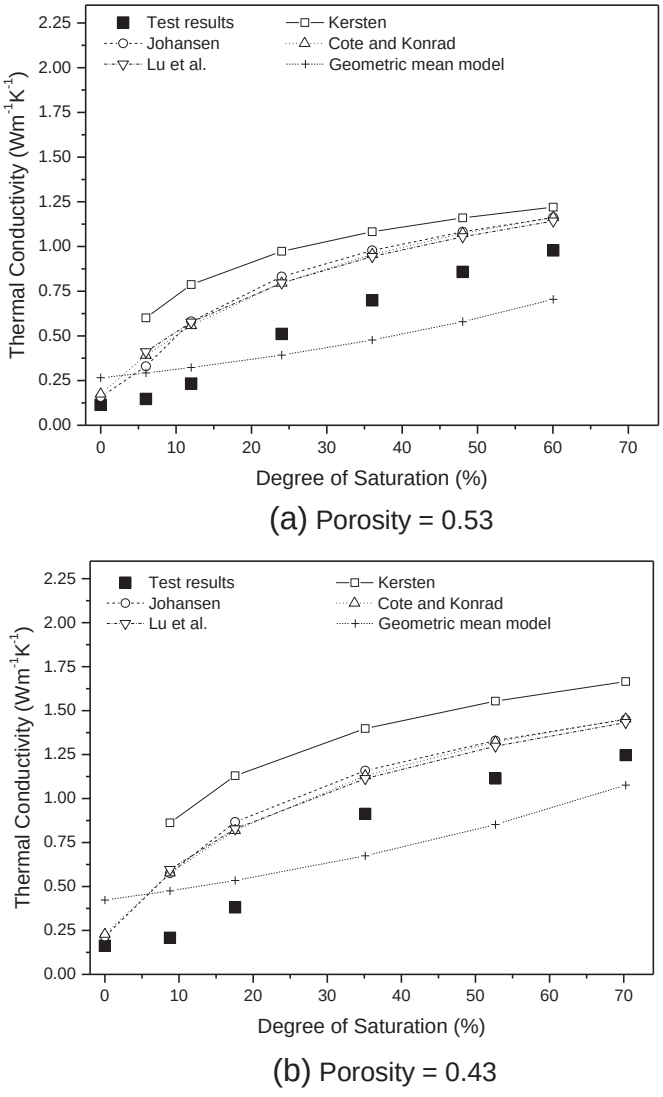

Fig. 3. Comparison results of experiments with previous prediction models.

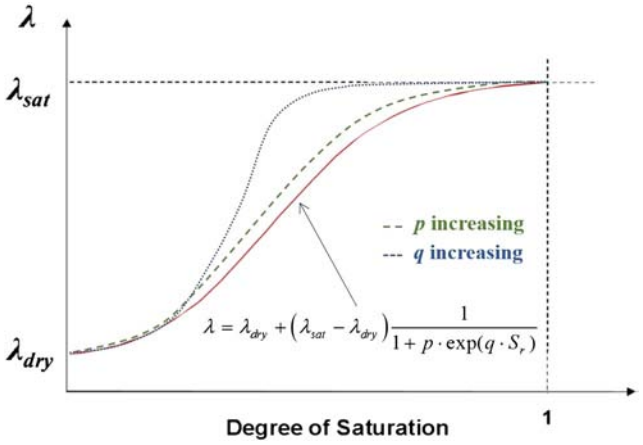

Fig. 4. Reliable thermal conductivity estimation model for unsaturated weathered granite soil.

2. Materials and methods

2.1. Thermal conductivity test and soil properties

In this study, a typical needle probe device, TP08 [35], was used to measure the soil thermal conductivity. This is because it has a short measurement time, which is a great advantage in developing a database of thermal properties. Once heat is injected by the needle probe, it induces a thermo-electromotive force, after which the thermal conductivity can be measured in a non-steady state. Fig. 1 shows a schematic diagram of an entire thermal conductivity test. Choi [36] developed a new probe system combined with a volumetric pressure extractor, in order to measure soil thermal conductivity and SWCC (soil-water characteristic curve) simultaneously. In this study, we used this measuring setup and investigated how the degree of saturation affects the soil thermal conductivity. The test was conducted according to ASTM D2325-68.

Soil samples were taken from representative areas in South Korea. The basic properties of samples such as porosity, specific gravity, and particle mineral composition were investigated. Thus, 162 data from eight regions in Korea (SJ: Seoul Jeungneung [37], KP: Kangwon Pyungchang, KI: Kangwon Inje, KT: Kangwon Taeback, BG: Busan Geumjung, SY: Sejong Yungi, CD: Chunnam Damyang, CY: Chunnam Yeosu) were collected for this study. In addition, to investigate the particle mineral composition of each soil sample, mineral quantitative analyses were conducted using the X-ray diffusion (XRD) method (Fig. 2). Hence, the particle thermal conductivities were finally obtained from a mixed model as shown in Table 1.

2.2. Prediction model

It has been found from earlier study that water content greatly influences the soil thermal conductivity [15,25,39–42], because the water content is strongly related to the contact area available for heat transfer between soil particles. In this study, the thermal conductivity of each soil was measured in a series of increasing volumetric water content (saturation process). As summarized in Table 2, the prediction models

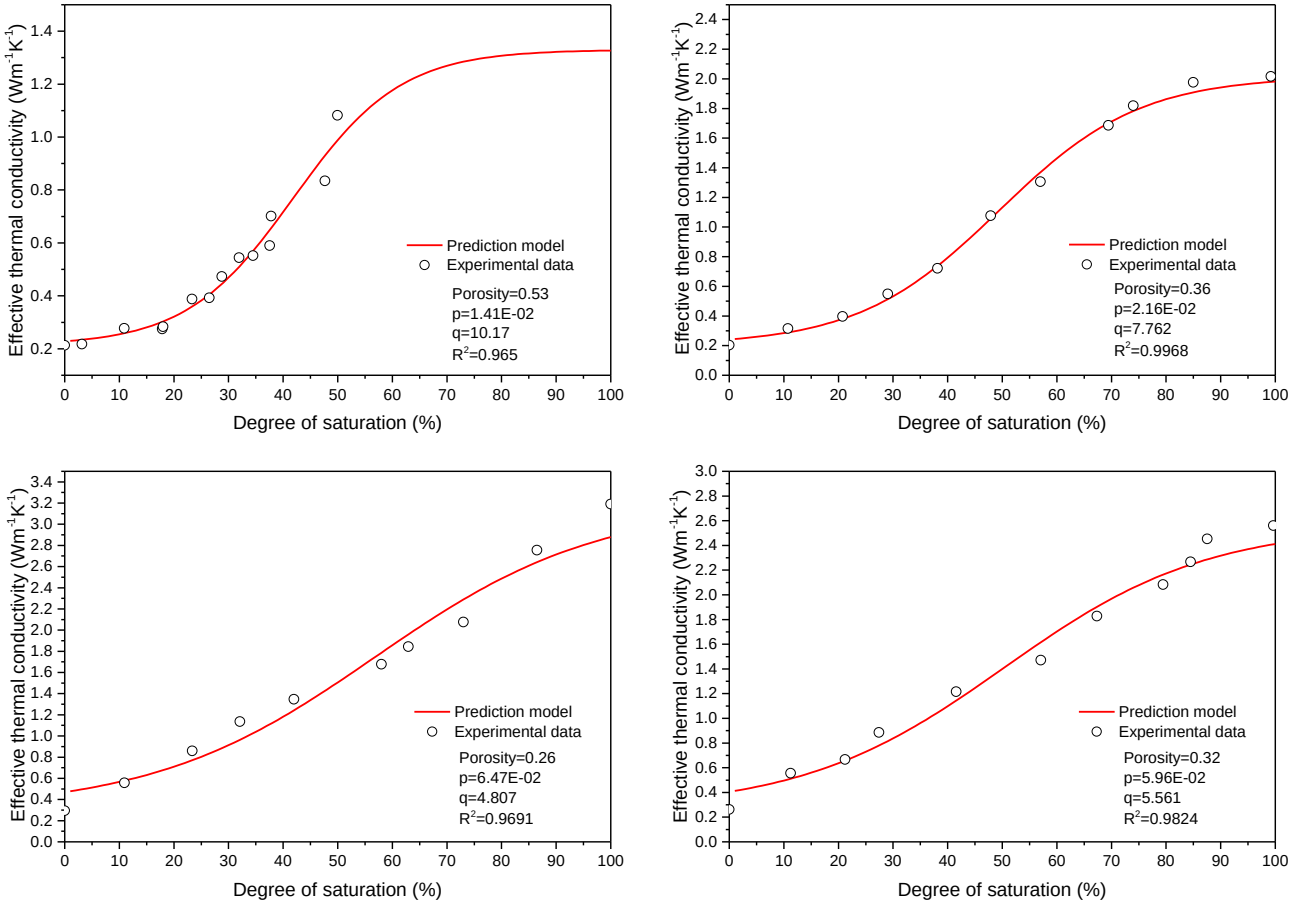

Fig. 5. Comparison results of experiments and newly developed prediction model.

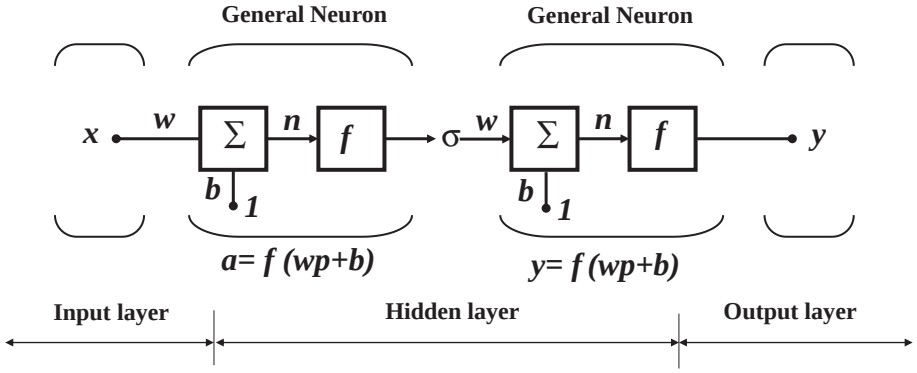

Fig. 6. Feed forward network of ANN model.

of Kersten [15], Johansen [16], Côté and Konrad [19], Lu et al. [20], and the geometric-mean-based model were used to analyze the test results. Fig. 3 shows the results from comparison of the experiments and prediction models. For weathered granite soils, the models of Johansen, Kersten, and Côté and Konrad, generally overestimated the thermal conductivity compared to the test results, while the geometric-mean-based model overestimated at low moisture levels, and underestimated at high moisture levels. Because the previous prediction models are applicable only to certain types of soil, these models did not provide predictions with a high degree of accuracy. Accordingly, our study was focused on developing a new prediction model, based on experimental databases that might be particularly applicable to weathered granite soils.

$$\lambda_{eff} = \lambda_{sat} + (\lambda_{dry} - \lambda_{sat}) \cdot \frac{1}{1 + p \cdot \exp(q \cdot S_r)} \quad (1)$$

The new prediction model (Eq. (1)) has lower and upper bounds, and the value varies with degree of saturation (Fig. 4). The lower bound (λ_{dry}) and upper bound (λ_{sat}) can be obtained from several mixed models such as arithmetic, harmonic and geometric mean. Moreover, p and q are the curve-fitting coefficients that determine the shape of the graph; coefficient p plays a role in movement of the x-intercept, while coefficient q is related to the slope of the graph. As shown in Fig. 5, the new prediction model was in good agreement with the experimental results for all moisture levels tested, and the curve fitting coefficient p and q could finally be determined. In fact, however, it is not easy to determine these coefficients unless experiments are conducted. To make the model more practical, an alternative that could estimate the coefficient p and q values without experiments was required. Accordingly, in this paper we propose the use of an artificial neural network model that can directly predict the p and q values given only information about the soil properties.

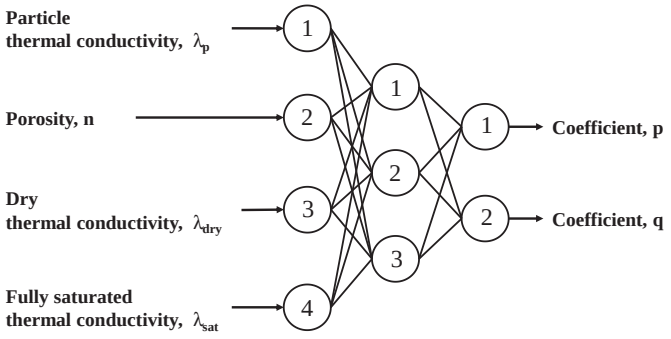

Fig. 7. Artificial neural network model for estimating the coefficients p and q.

3. Prediction of coefficients using an artificial neural network

3.1. Artificial neural network

An artificial neural network (ANN) is a computational technique capable of mapping and capturing all features and sub-features embedded in a large set of data, and that yields a certain output. The ANN handles imperfect or incomplete data, and captures nonlinear and complex relationships among variables of a system. For these abilities, the ANN has been recognized as a powerful tool for modeling.

As shown in Fig. 6, nodes in a feed forward network are generally arranged in layers, starting from a first input layer and ending at the final output layer. The input layer provides information to the network. In the hidden layer, which is placed between the input and output layer, each node multiplies every input by its interconnection weight, sums the product, and then passes the sum through a transfer function to produce its result. Finally, the output layer consists of values predicted by the network and, thus, represents the nodal output.

The number of hidden layers and the number of nodes in each hidden layer are usually determined by trial-and-error. Each neuron/node is an independent computational unit, which works according to the following formula:

$$y_j = f\left(\sum w_{ij} x_i + \theta_j\right) \quad (2)$$

Table 3
Data sets of soil properties and the empirical coefficients used for training.

Region	λ_p	n	λ_{dry}	λ_{sat}	p	q	Reference
SJ1	3.572	0.260	0.3020	3.190	0.0618	4.896	Lee [37]
SJ2	3.572	0.320	0.2616	2.560	0.0664	5.386	
SJ3	3.572	0.360	0.2032	2.020	0.0216	7.762	
KP1	3.491	0.431	0.1630	1.215	0.0244	13.020	
KP2	3.491	0.487	0.1840	1.445	0.0277	8.967	
KP3	3.491	0.526	0.1140	1.245	0.0635	7.649	
KP4	3.491	0.534	0.2130	1.330	0.0141	10.170	
KP5	3.491	0.575	0.1930	1.233	0.0147	9.796	
KI1	4.216	0.509	0.1510	1.052	0.0978	6.784	
KI2	4.216	0.590	0.1130	1.118	0.0379	8.138	
KT1	4.036	0.476	0.2090	0.917	0.0524	6.257	
KT2	4.036	0.581	0.1270	0.533	0.0181	16.900	
BG1	3.875	0.483	0.1510	2.174	0.0776	3.599	
BG2	3.875	0.565	0.1120	1.409	0.0980	3.475	
BG3	3.875	0.605	0.1850	1.215	0.0301	9.304	
SY1	3.504	0.479	0.1480	1.331	0.1020	5.875	
SY2	3.504	0.561	0.1050	1.193	0.0476	9.120	
SY3	3.504	0.558	0.1800	1.272	0.0400	8.684	
CD1	6.044	0.568	0.1941	1.581	0.0438	7.907	
CD2	6.044	0.607	0.2069	1.441	0.0178	10.110	
CD3	6.044	0.668	0.1183	1.248	0.0140	10.580	
CY1	4.750	0.555	0.1810	1.465	0.0764	6.324	
CY2	4.750	0.501	0.2370	1.641	0.0669	7.876	

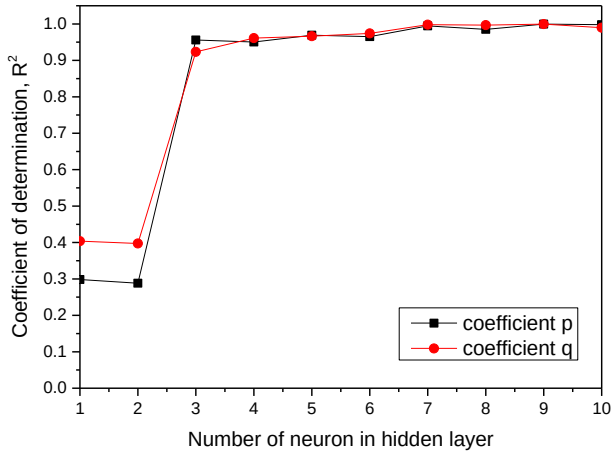

Fig. 8. Relationship between R^2 value and number of neurons in the hidden layer.

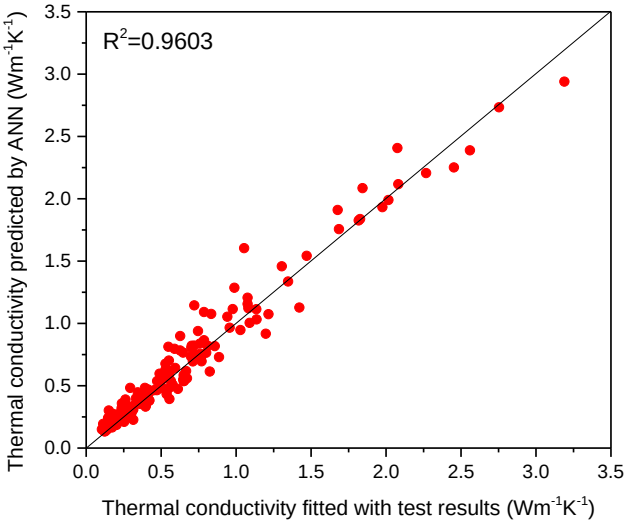

Fig. 10. Comparison of effective thermal conductivity obtained by test results and ANN.

where $y_j =$ the transformed output by the j^{th} hidden or output neuron, $x_i =$ the input of the i^{th} neuron in the previous layer, $w_{ij} =$ the weight of the connection joining the j^{th} neuron in a layer with the i^{th} neuron in the previous layer, $\theta_j =$ the bias at the j^{th} neuron, and $f =$ the transfer function that controls the output of a neuron, or squashes it to a finite range $(-1, 1)$. The weight indicates the strength of the connection while the bias increases the net input to the transfer function, leading to an increase in error convergence.

One of the main problems that occur during training of a neural network is called overfitting. Although the error of a training set is driven to a very small value, as new data are presented to the network, the error can become large. This phenomenon occurs more often when data are insufficient. To minimize the overfitting problem, Bayesian regularization can be applied to a back-propagation neural network [43,44]. This regularization technique considers the goodness of fit, as well as the network architecture, and a short description of it follows. Typically, training aims to reduce the sum of squared errors $F = E_D$. However, regularization adds an additional term, and the objective function becomes $F = \beta E_D + \alpha E_W$, where E_W is the sum of squares of the network weights, and α and β are objective function parameters. The relative size of the objective function parameters dictates the emphasis for training. If $\alpha \ll \beta$, then the training algorithm will drive the errors smaller. If $\alpha \gg \beta$, training will emphasize weight size reduction at the expense of network errors, thus producing a smoother network response [45].

3.2. Application of ANN to the prediction of unsaturated thermal conductivity

Herein, we developed a new thermal conductivity prediction model having two empirical coefficients, and these can be estimated using the artificial neural network model (ANN) shown in Fig. 7. We considered four major parameters (i.e., particle thermal conductivity, porosity, dry thermal conductivity, and fully saturated thermal conductivity) as input parameters in the ANN model for predicting the coefficient value p and q. Thus, twenty-three coefficient data sets (Table 3) were collected and evaluated using the neural network. Bayesian regularization was applied to a back-propagation neural network for prediction.

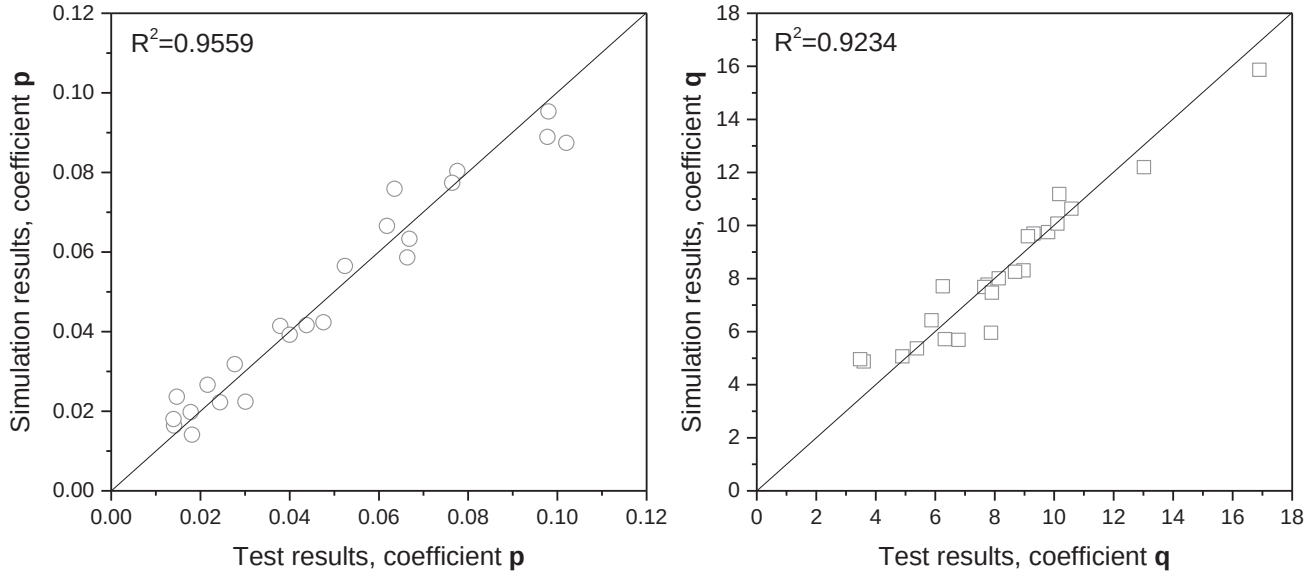

Fig. 9. Comparison of the results obtained by ANN model and experimental tests.

Table 4
Data sets of soil properties and the empirical coefficients for testing.

Region	λ_p	n	λ_{dry}	λ_{sat}	p	q
BG4	3.875	0.642	0.1480	1.132	0.0294	9.312
CN1	5.053	0.447	0.3400	1.904	0.0050	17.090
CN2	5.053	0.520	0.2320	1.623	0.0585	7.256
CN3	5.053	0.486	0.2400	1.752	0.0678	5.926
CI1	4.914	0.569	0.1800	1.443	0.0369	8.113
CI2	4.914	0.514	0.2120	1.625	0.0573	5.932

CN: Chunnam Namwon. CI: Chunnam Imsil.

In general, it is useful to scale the inputs and targets before training so that they always fall within a specified range [46]. In this study, the inputs and targets were scaled to fall in the range $[-1, 1]$. In other words, the minimum values of the original inputs and targets are scaled to '−1' and the maximum values of the original inputs and target are scaled to '1', respectively. After the network has been trained, vectors that contain the minimum and maximum values of the original inputs and targets should be used to transform any future inputs applied to the network, just like the network weights and biases. Then the network will be trained so that its output falls within the range $[-1, 1]$, and then these outputs are converted back into the same units used for the original targets. Whenever the trained network is used with new input, it should be preprocessed with the minimum and maximum values computed for the training set. Meanwhile, the transfer function in the first layer is the log-sigmoid function ($a = 1/(1 + e^{-n})$), and the second (output) layer transfer function is the tan-sigmoid function ($a = 2/(1 + e^{-2n})^{-1}$).

As shown in Fig. 7, the ANN model developed in this study has a 4–3–2 structure. It means that the model has four nodes in the input layer, three nodes in the hidden layer, and two nodes in the output layer. Fig. 8 shows the relationship between the R^2 value and the number of neurons in the hidden layer, in which R^2 is converging to a high value (>0.9) for both coefficient p and q when the model has more than three neurons in the hidden layer. This is the reason that the model has three neurons in the hidden layer. Fig. 9 shows the results simulated by the ANN model, and those obtained from the tests, regarding the coefficients p and q. For both p and q, the model shows overall high accuracy and does not represent a biased distribution. After this finding, these estimated coefficients could be applied to the thermal conductivity prediction model (Eq. (1)). Fig. 10 shows a comparison of the effective thermal conductivity obtained by the prediction model, with the test results and the neural network simulation at various degrees of water saturation. According to the results, the model showed that it could ensure an R^2 of 0.96 in predicting effective thermal conductivities without any biased distributions.

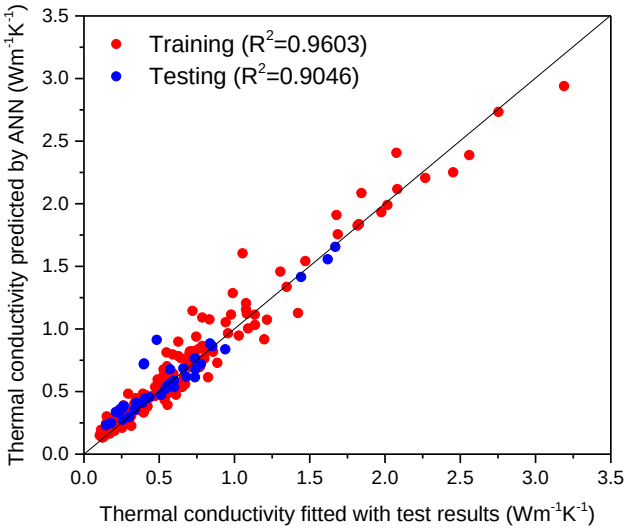

Fig. 12. Comparison of effective thermal conductivity obtained from test results and by the ANN (testing).

4. Verification of the trained network model

To evaluate the applicability of the trained network model, the model was tested to predict the coefficients p and q for data sets that had not been introduced during the training stage. Thus, six new data sets were used for testing the network model (Table 4). As can be seen in Fig. 11, the trained network model represented reasonable prediction results from the new testing data ($R^2 > 0.80$). The effective thermal conductivity was computed using coefficients p and q predicted by the ANN model, and then compared with the experimental test results, as shown in Fig. 12. The ANN model demonstrated a reliable accuracy ($R^2 = 0.9046$) in predicting the effective thermal conductivity, even when it used test data sets that were not part of the training data set. The results predicted by the ANN model for each test sample are shown in Fig. 13. It appears that the model traces the measured data curve with fairly good agreement, depending on the sample porosity, regional characteristics (especially mineral composition), and degree of saturation. These results suggest that the proposed prediction

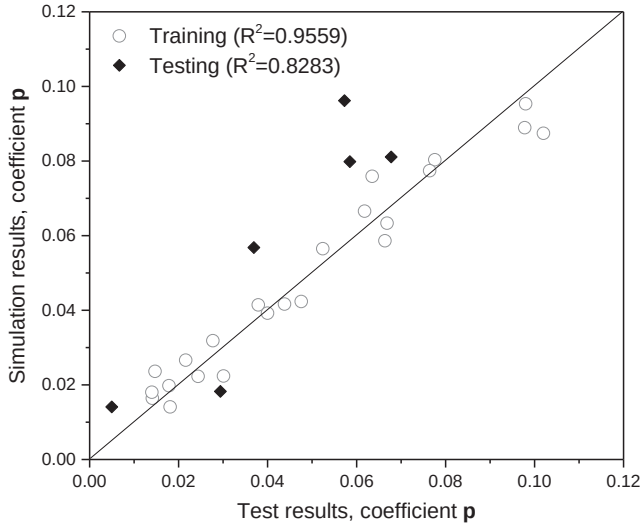

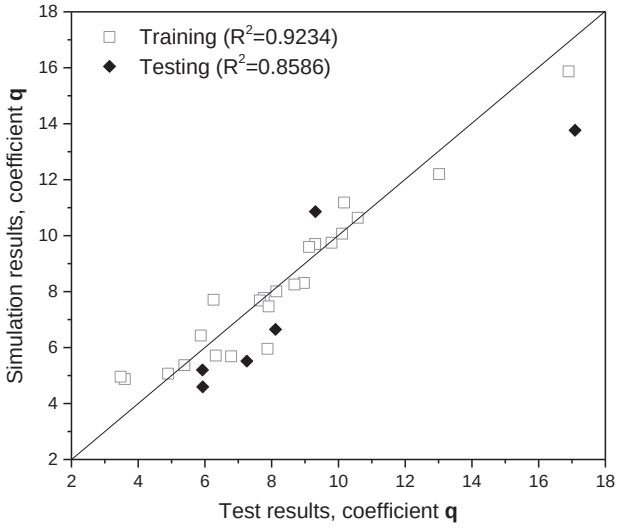

Fig. 11. Comparison of the results obtained by ANN model and experimental tests (testing).

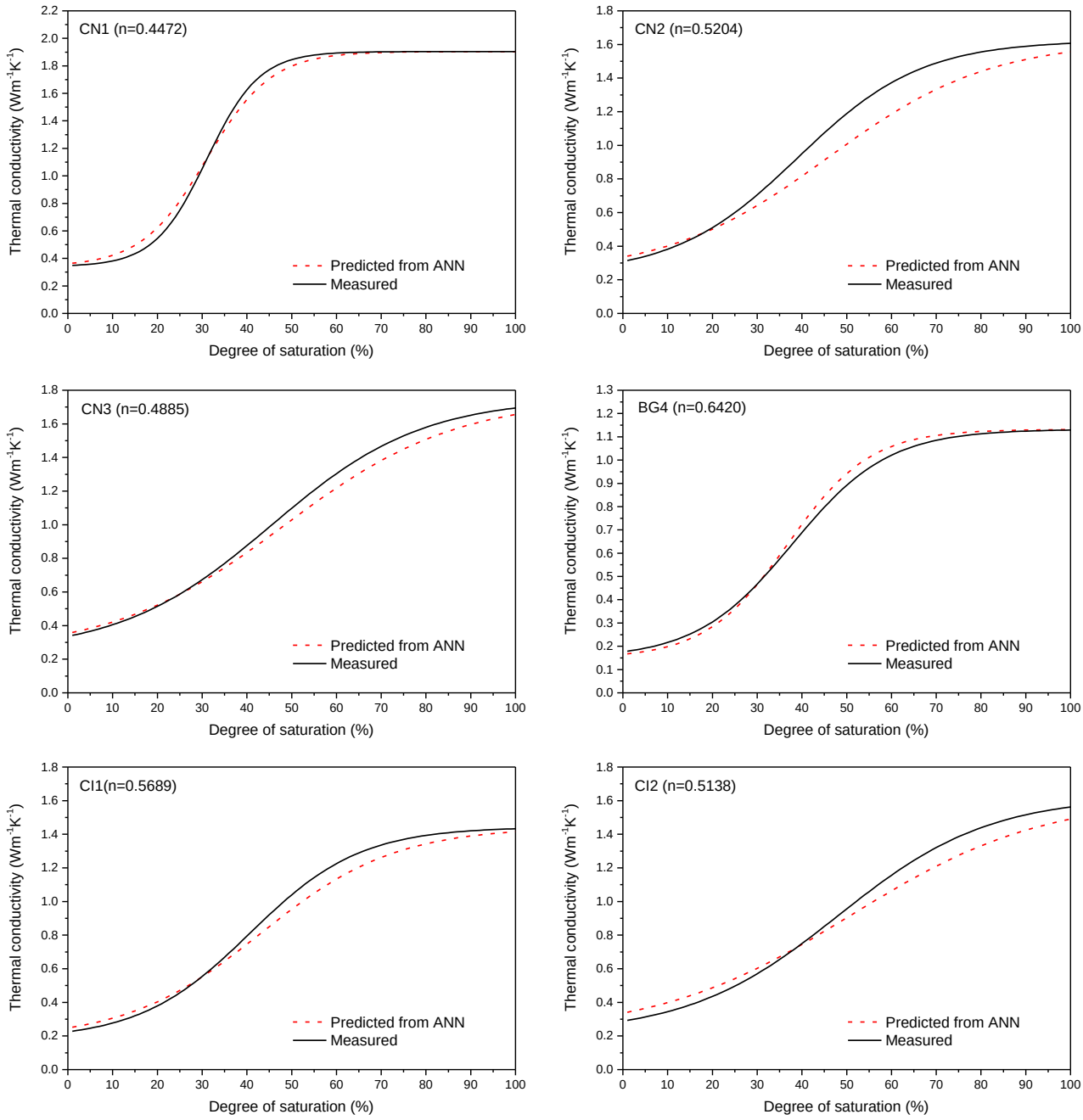

Fig. 13. Prediction results of the ANN model for each test sample.

model using ANN is reliable and applicable for predicting the effective thermal conductivity of unsaturated weathered granite soils. Table 5 provides the weights and biases used for the trained ANN model, so that others may make practical use of the model.

Table 5
Weights and biases for the trained ANN model.

	First layer			Second layer	
Weight	−4.0328	0.3925	2.5518	−5.3687	2.0435
	−5.5608	3.9487	3.0511	−7.5233	3.3124
	4.2562	1.1458	1.6304	5.5287	−3.2771
	6.6301	−1.8604	3.8811		
Bias	−0.3159			0.0847	
	−1.3158			0.2039	
	5.0057				

5. Summary and conclusions

In this study, a new empirical model for predicting thermal conductivity was presented that was based on experimental databases particularly applicable to unsaturated weathered granite soils. The proposed prediction model has two empirical coefficients, and these coefficients could be obtained from a newly developed artificial neural network model given only the information about the soil properties. To evaluate the applicability of the network model, the model was tested with data sets that had not been introduced during the training stage. The main conclusions drawn from the study results can be summarized as follows.

1. An accurate prediction of effective thermal conductivity of unsaturated soil is important for several heat transfer applications. In this study, a reliable method able to predict effective thermal conductivity with regard to the degree of saturation was proposed.

2. The newly developed prediction model has two empirical coefficients that can be estimated by the artificial neural network (ANN) model. Four major parameters (particle thermal conductivity, porosity, dry thermal conductivity, and fully saturated thermal conductivity) were considered input parameters, and twenty-three coefficient data sets were used for developing the trained neural network. Bayesian regularization was applied to a back-propagation neural network for prediction.
3. Because the trained neural network model showed reliable accuracy when having three or more neurons in the hidden layer, that is the number of neurons used in the hidden layer; hence, the ANN model has a 4–3–2 structure. The weights and biases corresponding to this structure were also presented so that others can use the trained ANN model more easily. The trained network model shows overall high accuracy and it does not represent a biased distribution in predicting the empirical coefficients. Moreover, the effective thermal conductivity obtained by the prediction model with the neural network simulation showed reliable accuracy ($R^2 = 0.96$).
4. In order to evaluate the applicability of the trained network model, the model was tested with data sets that had not been introduced during the training stage. According to the verification results, the trained network model demonstrated a reliable accuracy ($R^2 = 0.9046$) in predicting effective thermal conductivity, even when the model used test data sets that were not part of the training data sets. Moreover, the model results traced the measured data curve with fairly good agreement, depending on the sample porosity, regional characteristics, and degree of saturation. These results imply that the proposed prediction model using ANN is reliable and applicable for predicting the effective thermal conductivities of unsaturated, weathered granite soils.

Acknowledgements

This work was financially supported as a Basic Research Project of the National Research Foundation of Korea, under the Ministry of Science, ICT and Future Planning (grant no. 2013R1A2A2A01067898) and by grant 15RDRP-B076564-02 from the Regional Development Research Program funded by the Ministry of Land, Infrastructure and Transport of the Korean government.

References

[1] J.E. Bose, J.D. Parker, F.C. MacQuison, Design/Data Manual for Closed-Loop Ground Coupled Heat Pump System, Oklahoma State University for ASHRAE, 1985.
[2] G.H. Go, S.R. Lee, S. Yoon, H.B. Kang, Design of spiral coil PHC energy pile considering effective borehole thermal resistance and groundwater advection effects, Appl. Energy 125 (2014) 165–178.
[3] W. Zhang, H. Yang, P. Cui, L. Lu, N. Diao, Z. Fang, Study on spiral source models revealing groundwater transfusion effects on pile foundation ground heat exchangers, Int. J. Heat Mass Transf. 84 (2015) 119–129.
[4] Y. Xiang, H. Su, W. Gou, Y. Zhao, W. Kuang, Z. Liu, Y. Wu, A new practical numerical model for the energy pile with spiral coils, Int. J. Heat Mass Transf. 91 (2015) 777–784.
[5] D. Pahud, A. Fromentin, M. Hubbuch, Heat exchanger pile system for heating and cooling at Zürich airport, IEA Heat Pump Centre Newslett 17 (1) (1999) 15–16.
[6] L. Laloui, M. Moreni, L. Vulliet, Behavior of a dual-purpose pile as foundation and heat exchanger, Can. Geotech. J. 40 (2) (2003) 388–402.
[7] H. Brandle, Energy foundations and other thermo-active ground structures, Géotechnique 56 (2) (2006) 81–122.
[8] P. Cui, X. Li, Y. Man, Z. Fang, Heat transfer analysis of pile geothermal heat exchangers with spiral coils, Appl. Energy 88 (2011) 4113–4119.
[9] O. Boennec, Shallow ground energy systems, Energy 161 (2008) 57–61.
[10] P.M. Congedo, G. Colangelo, G. Starace, CFD simulation of horizontal ground heat exchangers: a comparison among different configurations, Appl. Therm. Eng. 33 (3–4) (2012) 24–32.
[11] E. Pulat, S. Coskun, K. Unlu, N. Yamankaradeniz, Experimental study of horizontal ground source heat pump performance for mild climate in Turkey, Energy 34 (2009) 1284–1295.
[12] G. Florides, E. Theofanous, I. Iosif-Stylianou, S. Tassou, P. Christodoulides, Z. Zomeni, E. Tsiolakis, S. Kalogirou, V. Messaritis, P. Pouloupatis, G. Panayiotou, Modeling and assessment of the efficiency of horizontal and vertical ground heat exchangers, Energy 58 (2013) 655–663.
[13] Ş. Bozdağ, B. Turgut, H. Paksoy, D. Dikici, M. Mazman, H. Evliya, Ground water level influence on thermal response test in Adana, Turkey, Int. J. Energy Res. 32 (2008) 629–633.
[14] M. Preene, W. Powrie, Ground energy systems: from analysis to geotechnical design, Geotechnique 59 (3) (2009) 261–271.
[15] M.S. Kersten, Laboratory research for the determination of the thermal properties of soils, Arctic construction and frost effects laboratory, Technical Report 23 (1949).
[16] O. Johansen, Thermal Conductivity of Soils, University of Trondheim, 1975 (Ph.D. Thesis).
[17] F. Donazzi, E. Occhini, A. Seppi, Soil thermal and hydrological characteristics in designing underground cables, Proc. IEE 126 (6) (1979) 506–516.
[18] O. Farouki, Evaluation of methods for calculating soil thermal conductivity, CRREL Report 82-8 (March 1982).
[19] J. Côté, J.M. Konrad, A generalized thermal conductivity model for soils and construction materials, Can. Geotech. J. 42 (2) (2005) 443–458.
[20] S. Lu, T. Ren, Y. Gong, An improved model for predicting soil thermal conductivity from water content at room temperature, SSSA J. 71 (1) (2007) 8–14.
[21] S.X. Chen, Thermal conductivity of sands, Heat Mass Transf. 44 (10) (2008) 1241–1246.
[22] A. Gemant, The thermal conductivity of soils, J. Appl. Phys. 21 (8) (1950) 750–752.
[23] D.A. De Vries, Thermal properties of soils. In Physics of the Plant Environment (Ed. W. R. Van Wijk), Pp. 210–235. New York: John Wiley & Sons; 1963.
[24] E. Penner, Thermal conductivity of frozen soils, Can. J. Earth Science 7 (1970) 982–987.
[25] E. Penner, G.H. Johnston, L.E. Goodrich, Thermal conductivity laboratory studies of some Mackenzie Highway soils, Can. Geotech. J. 12 (3) (1975) 217–288.
[26] F. Gori, A theoretical model for predicting the effective thermal conductivity of unsaturated frozen soils, Proceedings of the 4th International Conference on Permafrost 1983, pp. 363–368 Fairbanks. USA.
[27] F. Gori, C. Marino, M. Pietrafesa, Experimental measurements and theoretical predictions of the effective thermal conductivity of porous saturated two phases media, Int. C. Heat and Mass Transfer 28 (8) (2001) 1091–1102.
[28] F. Gori, S. Corasaniti, Experimental measurements and theoretical prediction of the thermal conductivity of two-and three-phase water/olivine systems, Int. J. Thermophysics 24 (5) (2003) 1339–1353.
[29] V.R. Tarnawski, F. Gori, B. Wagner, G.D. Buchan, Modelling approaches to predicting thermal conductivity of soils at high temperatures, Int. J. Energy Res. 24 (5) (2000) 403–423.
[30] F. Gori, S. Corasaniti, Theoretical prediction of the soil thermal conductivity at moderately high temperatures, J. Heat Transf. 124 (6) (2002) 1001–1008.
[31] S.K. Haigh, Thermal conductivity of sands, Geotechnique 62 (7) (2012) 617–625.
[32] F. Gori, S. Corasaniti, New model to evaluate the effective thermal conductivity of three-phase soils, Int. C. Heat and Mass Transfer 47 (2013) 1–6.
[33] F. Gori, Prediction of effective thermal conductivity of two-phase media (including saturated soils), Proceedings of the XVI International Congress of Refrigeration, Paris B1-26 (1983) 525–531.
[34] F. Gori, S. Corasaniti, Effective Thermal Conductivity of Three-Phase Soils, Proceedings of ASME 2012 International Mechanical Engineering Conference and Exposition, IMECE2012-86304, Houston, Texas, USA, 2012.
[35] Hukseflux. User manual of TP08: small size non-steady probe for thermal conductivity measurement. Hukseflux Thermal Sensors. DelftNetherlands 2006.
[36] J.C. Choi, Numerical simulation on the performance of energy pile considering effect of unsaturated soil condition, KAIST, 2011 (Ph.D. Thesis).
[37] K.J. Lee, Study on Thermal Characteristics of Backfill Materials for Horizontal Ground Heat ExchangerMaster Thesis Korea University, 2010.
[38] K. Horai, Thermal conductivity of rock-forming minerals, J. Geophys. Res. 76 (5) (1971) 1278–1307.
[39] N.H. Abu-Hamdeh, R.C. Reeder, Soil thermal conductivity: effects of density, moisture, salt concentration, and organic matter, Soil Sci. Soc. Am. J. 64 (2010) 1285–1290.
[40] E. Sikora, J. Kossowski, Thermal conductivity and diffusivity estimations of uncompacted and compacted soils using computing methods, Polish, J. Soil Sci. 26 (1) (1993) 19–26.
[41] B. Usowicz, J. Kossowski, P. Baranowski, Spatial variability of soil thermal properties in cultivated fields, Soil Till. Res. 39 (1996) 85–100.
[42] L.A. Salomone, W.D. Kovacs, Thermal resistivity of soils, J. Geotech. Eng. 110 (3) (1984) 375–389.
[43] D.J.C. MacKay, A practical Bayesian framework for backpropagation networks, Neural Comput. 4 (3) (1992) 448–472.
[44] D.J.C. MacKay, Bayesian interpolation, Neural Comput. 4 (3) (1992) 415–447.
[45] F.D. Foresee, M.T. Hagan, Gauss–Newton approximation to Bayesian learning, Proceedings of the International Joint Conference on Neural Networks (1997) 1930–1935.
[46] M.Y. Rafiq, G. Bugmann, D.J. Easterbrook, Neural network design for engineering applications, Comput. Struct. 79 (2001) 1541–1552.